Bone 45 (2009) 1175–1185

Contents lists available at ScienceDirect

Bone

journal homepage: www.elsevier.com/locate/bone

Chloride intracellular channel 1 regulates osteoblast differentiation

Jae-Yeon Yang [a], Ju Yeon Jung [a], Sun Wook Cho [a], Hyung Jin Choi [a], Sang Wan Kim [a], Seong Yeon Kim [a], Hee Joong Kim [b], Chang Han Jang [c], Min Goo Lee [d], Jin Han [c], Chan Soo Shin [a,*]

[a] Department of Internal Medicine, Seoul National University College of Medicine, 101 Daehak-Ro, Jongno-Gu, Seoul 110-744, Korea
[b] Department of Orthopedic Surgery, Seoul National University College of Medicine, Seoul, Korea
[c] National Research Laboratory for Mitochondrial Signaling, Department of Physiology, College of Medicine, Cardiovascular and Metabolic Disease Center, FIRST Mitochondrial Research Group, Inje University, Busan, Korea
[d] Department of Pharmacology, Yonsei University College of Medicine, Seoul, Korea

ARTICLE INFO

Article history:
Received 30 May 2009
Revised 14 August 2009
Accepted 17 August 2009
Available online 22 August 2009

Edited by: R. Baron

Keywords:
Osteoblast
Wnt
Chloride intracellular channel
Mitochondria
Differentiation

ABSTRACT

We have identified chloride intracellular channel 1 (CLIC1) through proteomic approach, which was increased in response to canonical wnt signaling while being almost shut-off by adipogenic treatment in mouse mesenchymal C3H10T1/2 cells. We found that CLIC1 was expressed in mouse (MC3T3-E1), rat (ROS 17/2.8 and UMR-106) or human (MG63 and SaOS2) osteoblastic cell lines as well as primary culture of mouse calvarial cells by RT-PCR or Western blot analysis. The expression level of CLIC1 is increased upon treatment of osteogenic medium, whereas it almost disappeared in adipogenic condition, confirming the proteomic data. The expression of CLIC1 was localized mainly in nuclear membrane and vesiculo-cytoplasmic, the latter of which was colocalized with mitochondria. Retroviral overexpression of CLIC1 did not increase whole-cell current but induces hyperpolarization of mitochondrial membrane potential estimated using the fluorescent dye TMRE. Moreover, overexpression of CLIC1 resulted in increase in osteoblastic differentiation of C3H10T1/2 cells as measured by ALP activities or osteoblastic gene expression (osterix, ALP and osteocalcin), although it did not result in induction of Runx2 transcription activities at mouse osteocalcin (OG2) promoter. Finally, *in vitro* knock-down of CLIC1 using stable siRNA CLIC1 significantly suppressed osteoblastic differentiation. Taken together, these results suggest that CLIC1 may play a role in the regulation of osteoblastic differentiation from mesenchymal progenitors, although its physiologic role in osteoblasts remains to be determined.

Introduction

Wnt proteins constitute a family of secreted proteins involved in development and maintenance of a variety of organs and tissues, including bone. Activation of wnt signaling occurs upon binding of wnt ligands to receptor complex composed of the 7-transmembrane domain-spanning frizzled receptor and either low-density lipoprotein receptor-related protein 5 or 6 (LRP5/6) (for review see ref. [1]). Involvement of Wnt signaling in the regulation of bone mass was evidenced by cases of osteoporosis–pseudoglioma syndrome, in which loss-of-function mutations in human LRP5 genes resulted in low bone mineral density and skeletal fragility [2]. In contrast, point mutations in LRP5 are associated with extremely high bone density in an autosomal dominant inheritance pattern [3]. *In vitro*, stable expression of Wnt1, Wnt3a, Wnt6 or Wnt7b enhanced the growth rate of C3H10T1/2 cells, a pluripotent mesenchymal precursor cell line [4]. Moreover, Wnt-1, Wnt-2, and Wnt-3a induced alkaline phosphatase (ALP) activity, the early marker of osteoblastic differentiation, in C2C12, C3H10T1/2, and ST2 cells [2,5]. In addition, Wnt proteins also play a role in the lineage allocation of mesenchymal precursors as demonstrated by recent studies that showed inhibition of adipogenesis from preadipocytes by Wnt-1a and Wnt-10b [6] and increased bone volume and decreased fat tissue in Wnt-10b over-expressing transgenic mice[7]. These studies demonstrate that Wnts stimulate growth and maturation of osteoblast precursors as well as drive mesenchymal cells to osteoblastic lineage.

Chloride intracellular channel (CLIC) proteins are a recently described family of proteins related to the bovine intracellular chloride channel p64 [8]. To date, seven distinct members of CLICs are identified: CLIC1, CLIC2, CLIC3, CLIC4, CLIC5, p64, and parchorin [9]. Although all of these proteins have been thought to be able to form anion channel in organellar or plasma membranes, these putative channel functions are controversial because they exist in both soluble and integral membrane forms [8]. Among the members of CLICs, CLIC1, which is expressed in most tissues and cell types, has been most extensively studied. The distribution of intracellular CLIC1 expression varies depending on the cell types, from intracellular vesicular pattern to intranuclear distribution [9]. Unlike other members of CLICs, CLIC1 seems to function as a real chloride channel

* Corresponding author. Fax: +82 2 765 3734.
E-mail address: csshin@snu.ac.kr (C.S. Shin).

8756-3282/$ – see front matter © 2009 Elsevier Inc. All rights reserved.
doi:10.1016/j.bone.2009.08.012

as evidenced by the increased chloride channel activity in plasma and nuclear membranes when transfected to cultured cells [10].

In an attempt to identify the mediators that could play a pivotal role in the lineage commitment from mesenchymal cells to osteoblast or adipogenesis, we explored new protein profiles by proteomic techniques. We found that CLIC1 is one of the Wnt-induced proteins up-regulated by more than ×1.3–1.8 times, while being shut-off by adipogenic treatment. Furthermore, overexpression of CLIC1 enhanced the osteogenic differentiation of C3H101/2 cells, a murine pluripotent mesenchymal cell line. We suggest that CLIC1 may be one of the mediators regulating the osteoblastic differentiation of the mesenchymal cells.

Material and methods

Materials

Polyclonal anti-CLIC1 antibody was purchased from AVIVA System Biology (San Diego, CA). Monoclonal mouse anti-HA antibody was obtained from Covance Inc. and polyclonal goat anti-mtTFA (mitochondrial transcription factor A) antibody was from Santa Cruz Biotechnology. IAA-94 was obtained from R and D systems. TRI reagent was from Invitrogen and Western blotting detection reagents from Amersham Biosciences. Random priming kits and reagents for the luciferase assay were purchased from Promega Corp. Lipofectamine Plus was obtained from Invitrogen Corp. Oligonucleotides were synthesized by Bioneer Corp.(Chungwon, Korea), and all other chemicals, including tissue culture medium, were from Sigma Chemical, unless otherwise indicated.

Cell culture

Mouse embryonic mesenchymal cells C3H10T1/2 (American Type Culture Collection, Manassas, VA), are pluripotent cells that retain an immature, fibroblast-like appearance under standard tissue culture conditions. C3H10T1/2 cells were grown in Dulbecco's modified Eagle's medium (DMEM) containing 10% FBS. During osteoblastic differentiation studies, C3H10T1/2 cells were cultured in DMEM medium containing 10% FBS supplemented with 50 μg/ml ascorbic acid and 10 mM β-glycerophosphate.

Mouse MC3T3-E1 (RIKEN cell bank, Tsukuba, Japan) osteoblastic cells were derived from spontaneously immortalized calvarial cells and represent immature osteogenic cells. Four osteosarcoma cell lines from rat (ROS 17/2.8 and UMR-106) and human (MG 63 and SaOS2) exhibit features of mature osteoblasts. All the experiments were performed using cells at passage 9–12. MC3T3-E1 cells were cultured in α-minimum essential medium (α-MEM) with 10% fetal bovine serum (FBS), ROS 17/2.8 and MG 63 cells in Dulbecco's modified Eagle's medium (DMEM) with 10% FBS, and SaOS2 cells in McCoy's 5A medium with 15% FBS at 37 °C in a humidified atmosphere of 5% CO_2 and 95% air. Normal mouse osteoblasts were isolated from 21-day fetal mouse calvariae using a well-characterized technique essentially as described previously as described [11]. Human bone marrow stromal cells (hBMSC) were obtained by aspiration from the iliac crest of subjects (23–78 years) undergoing hip prosthesis surgery due to non-necrotic hip disorders with ethical approval from Seoul National University Hospital [12] using a modification of the procedure described by Pittenger et al.[12,13].

Constructs

Retroviral vectors for Wnt-1a (pLXSN-Wnt-1a) and Wnt-10b (pLNCX2-Wnt-10b) were kindly provided by Dr. MacDougald (University of Michigan, Ann Arbor). CLIC1 (NCC27) cDNA construct, cloned in pIRES vector (Clontech) was obtained from Dr. Samuel Breit (University of New South Wales, Sydney, Australia). A hemagglutinin (HA) epitope was incorporated at the C-terminal of CLIC1 by PCR, and then ligated into the *Bgl*II/*Eco*RI site of pMSCV-IRES-GFP retroviral vector (a kind gift from Dr. Neil A. Clipstone at the Northwestern University) upstream of IRES, giving pMSCV-CLIC1-IRES-GFP. In order to generate fusion construct that contains GFP at the 3′ terminal of CLIC1, CLIC1 cDNA without stop codon was PCR amplified and ligated into the *Bgl*II-*Bst*X1 site of pEGFP-N1 yielding pCLIC1-EGFP.

Mouse osteocalcin II (OG2) promoter-luciferase reporter construct, -1.3 OG2-Luc, containing 1.3 kb segment (positions −1316 to +13) has been previously described [14].

CLIC siRNA construct

Short interfering RNA target sequences were designed against the mouse CLIC1 gene using siRNA Sequence Selector (BD Biosciences). We selected 3 target sequences specific for the mouse CLIC1 mRNA (GenBank™ accession number NM_033444): si610, AGCCCTGAAGGTTCTAGAC (610–628 bp); si753, AGCTTCACATAGTACAGGT (753–771); and si887, GAGATAGAGCTAGCCTATG (887–905 bp). Three pairs of complementary oligonucleotides were annealed and then inserted into the pSIREN-RetroQ vector (BD Biosciences) downstream of the human U6 promoter between *Bam*HI and *Eco*RI sites.

Retrovirus production and transduction of cell lines

For transient generation of VSV-G pseudo-typed retrovirus, 293T cells (a packaging cell line) were plated in 100-mm-diameter dishes (5×10^6 cells in 10 ml of DMEM containing 10% FBS) and allowed to attach overnight. The plasmids pMD-gag-pol and pMD-VSVG (both kindly provided by Dr. Richard C. Mulligan at Harvard Medical School, Boston, MA) and the retroviral vectors were introduced into 293T cells using Lipofectamine Plus reagents according to the manufacturer's instructions. Viral supernatant was collected at 48 h after DNA addition, filtered through a 0.45 μm syringe filter (Nalgene), and stored at -80 °C.

Logarithmically growing C3H10T1/2 cells were transduced with virus-containing supernatants in the presence of 4 μg/ml Polybrene for 5 h. Cells were collected 48–72 h later, and stable cells were selected using G418 (1000 μg/ml) for pLXSN-Wnt-1a and pLNCX2-Wnt-10b infection or puromycin (400 ng/ml) for pSIREN-RetroQ infection. For C3H10T1/2 cells transduced with pMSCV-CLIC1-IRES-GFP or pMSCV-IRES-GFP retrovirus, GFP-positive fractions were FACS-sorted using a BD FACS Vantage Cell Sorter and used for study.

Reverse transcription PCR

The mRNA expression of CLIC1 in cells was determined by RT-PCR analysis using ~2 μg of total RNA. The sequences of the primers used were described in Table 1. The reverse transcription was performed in a volume of 20 μl using SuperScript III First-Strand Synthesis System (Invitrogen). Then, PCR was accomplished in a final volume of 50 μl using HiQ Taq Red DNA Polymerase (GenDEPOT). The reaction

Table 1
Sequences of PCR primers used to amplify each of the genes in RT-PCR.

Gene	Primer	Sequences (5′ → 3′)	Product size (bp)
Mouse CLIC1	Forward	CTCTGGCTCAAGGGAGTCAC	275
	Reverse	AGGGCTGGGTTTGAGTTCTT	
Human CLIC1	Forward	CTCAGCTCTGAACCCTGAGTCC	346
	Reverse	TTGCTCAAGTACCGATGCAC	
Rat CLIC1	Forward	TACCCAAAGTTGGCTGCTCT	300
	Reverse	TTTgCACACCACCTGGACTA	

conditions were as follows; reverse transcription (one cycle), 25 °C for 10 min, 50 °C for 50 min and 85 °C for 5 min; PCR amplification (28 cycles), predenaturation at 94 °C for 3 min, denaturation at 94 °C for 20 s, annealing at 56 °C for 30 s, and extension at 72 °C for 40 s; and final extension (one cycle) at 72 °C for 5 min. The PCR products were electrophoresed in 1.5% agarose gel and visualized by ethidium bromide staining.

Real-time quantitative RT-PCR measurements of gene expression

The mRNA expressions of Runx2, osterix, ALP and osteocalcin were determined by real-time quantitative PCR (qPCR). cDNA synthesis was performed with 1 μg of total RNA using a Reverse Transcription System kit (Promega, Madison, WI). qPCR was performed by applying the real-time SYBR Green PCR technology with the use of an ABI PRISM 7900 HT sequence detection system (Applied Biosystems) using the sets of primers for genes listed in Table 2, including β-actin. Amplification reaction was performed in a 20 μl volume, using 2× Universal SYBR PCR Master Mix (PerkinElmer Life Sciences). The relative gene expressions were calculated by comparing the ratios to reference gene, β-actin cycle threshold (C_T). All PCR reactions were performed at least in duplicate.

Western blotting

Cell lysates were prepared by treating cells with lysis buffer (150 mM NaCl, 50 mM Tris–Cl (pH 7.4), 20 mM EDTA, 1% Triton X-100, 1% sodium deoxycholate, 0.1% SDS and protease inhibitors). Lysates were sonicated for 20 min on ice and centrifuged at 10,000*g* for 10 min to sediment particulate material and the supernatant was used for whole-cell lysates.

For subcellular fractionation, cells were scraped in ice-cold MIB buffer (10 mM Tris (pH 7.4), 250 mM sucrose, 1 mM EDTA), and gently homogenized using a glass tissue grinder (Wheaton, Millville, NJ). The homogenates were then fractionated at 4 °C as previously described [15]. Briefly, samples were first centrifuged at 700*g* for 5 minutes at 4 °C. The supernatants were collected and further centrifuged at 16,100*g* for 20 minutes at 4 °C. The second supernatants which contained cytosolic fraction were segregated from the pellet. The second pellet containing the mitochondrial fraction was washed to ice-cold MIB buffer and centrifuged at 16,100*g* for 20 minutes at 4 °C.

Protein concentrations were determined by the Bradford protein assay. SDS-polyacrylamide gel electrophoresis was performed on 12% polyacrylamide gels and the resolved proteins were transferred onto nitrocellulose membranes. Membranes were blocked with 0.1% Tween-20 PBS and 5% dry milk, at pH 7.4, for 1 h. Appropriate antibodies were added and incubation was continued overnight. After washing in 0.1% Tween-20 PBS, the membranes were incubated with horseradish peroxidase-conjugated anti-mouse antibodies for 1 h. After extensive washing, bands were visualized by chemiluminescence using an ECL kit.

Table 2
Sequences of PCR primers used for real time quantitative PCR.

Gene	Primer	Sequences (5′ → 3′)	PCR product size (bp)
Runx2	Forward	TTTAGGGCGCATTCCTCATC	102
	Reverse	TGTCCTTGTGGATTAAAAGGACTTG	
Osterix	Forward	TTTAAACAAACACGATGATGATGA	138
	Reverse	ATTGGACTTCCCCCTTCTTG	
ALP	Forward	TCAGGGCAATGAGGTCACATC	67
	Reverse	CACAATGCCCACGGACTTC	
Osteocalcin	Forward	GCGCTCTGTCTCTCTGACCT	89
	Reverse	ACCTTATTGCCCTCCTGCTT	
β-actin	Forward	TGGGTATGGAATCCTGTGGC	103
	Reverse	CCAGACAGCACTGTGTTGGC	

Alkaline phosphatase (ALP) assay

A semiquantitative method using α-naphthyl phosphate as a substrate and Fast Blue salt (Sigma) as diazonium salt was used. Briefly, cells were washed with phosphate-buffered saline (PBS), pH 7.4 and scraped immediately after adding 100 μl of 0.5% Triton X-100; the lysates were then sonicated for 20 s at 4 °C. Enzyme activity assay was performed in assay buffer (10 mM $MgCl_2$ and 0.1 M alkaline buffer, pH 10.3) containing 10 mM *p*-nitrophenylphosphate. Tubes were incubated in a 37 °C water bath and timed. The reaction was stopped by adding 0.3 N NaOH. Reaction mixtures were transferred into 96 wells plate, and absorbance was read at OD 405. Relative ALP activity is defined as millimoles of *p*-nitrophenol phosphate hydrolyzed per minute per milligram of total protein.

Alizarin Red stain

Matrix mineralization was assessed using Alizarin Red staining. The cells were fixed with 70% ethanol for 1 h at 4 °C. Fixed samples were washed three times with PBS, rinsed with deionized water, and then stained for 10 min with 40 mM Alizarin Red S solution (Sigma), pH 4.2 at room temperature.

Two-dimensional gel electrophoresis and gel staining

Protein samples of osteoblastic differentiation were obtained from lysates of C3H10T1/2 cells transduced with pLXSN , pLXSN-Wnt-1a or pLXCX2-Wnt-10b at 48 h after transduction. For adipogenic stimulation, C3H10T1/2 cells were treated with 5 μg/ml insulin, 0.5 mM IBMX, 0.1 μM dexamethasone for 48 h. Nonstimulated samples were used as a control. Two-dimensional gel electrophoresis was performed as previously described [16]. Briefly, 100 μg of protein from cell lysates was loaded to the IPG (immobilized, pH 3 to 10, nonlinear gradient) strips by in-gel rehydration with the use of IPGPhor (18 cm, Amersham Pharmacia Biotech). The first-dimensional isoelectric focusing was performed successively at 500 V for 1 h, 1000 V for 1 h, and 8000 V for 5 h. In the second dimension, the proteins were separated by size in a 7 to 17% T polyacrylamide gradient gel. Separation was continued at 10 mA per gel in running buffer (25 mmol/L Tris, pH 8.8, 198 mmol/L glycine, 0.1% SDS) until the BPB reached the bottom of the gel. After electrophoresis, the protein spots were visualized by using a modified silver-staining protocol compatible with MALDI TOF MS. The silver-stained gel was scanned with the use of a densitometer 800 (Bio-Rad), and the digitalized image was analyzed with the use of PDQUEST software (version 6.1, Bio-Rad).

Mass spectrometry

Proteins were identified by peptide mass finger printing methods [17] and ESI-MS/MS. The excised gel spots were destained with 100 μl of destain solution (30 mM potassium ferricyanide (Sigma), in 100 mM sodium thiosulfate (Merck), with shaking for 5 min. After the solution was removed, the gel spots were incubated with 200 mM ammonium bicarbonate for 20 min. The gel pieces were dried in a speed vacuum concentrator for 5 min and then rehydrated with 20 μl of 50 mM ammonium bicarbonate containing 0.2 μg modified trypsin for 45 min on ice. After removal of solution, 30 μl of 50 mM ammonium bicarbonate was added and the digestion was performed overnight at 37 °C. The peptides were desalted and concentrated using C18 nanoscale (porus C18) column. For the analysis of MALDI-TOF MS by peptide-mass fingerprinting method, the peptides were eluted by 0.8 μl of matrix solution (70 % acetonitrile, 0.1% TFA, 10 mg/ml alpha-cyano-4-hydroxycinamic acid). The eluted peptides were spotted onto a stainless steel target plate. Masses of peptides were determined using MALDI-TOF MS (Model M@LDI-R; Micromass, Manchester, UK).

Table 3
Quantitative analysis of proteins regulated by Wnt-1a, Wnt-10b, or adipogenic medium of C3H10T1/2 cells.

Genes	Accession number	Wnt-1a	Wnt-10b	Adipogenic
dihydropyrimidinase-like 2	Gi 40254595,	0.16	0.00	0.77
chloride intracellular channel 1	Gi 50657380,	1.34	1.86	0.00
Vat1 protein	Gi 55715891,	2.04	2.14	1.10
unnamed protein product	Gi 26346769,	3.44	1.61	0.34
PREDICTED: similar to insulin receptor substrate p53 short form	Gi 57099165	4.30	2.03	0.89
Pyruvate kinase, isozyme M2	Gi 2506796,	6.20	6.05	0.98

Calibration was performed using internal mass of trypsin auto digestion product (m/z 2211.105).

For analyses by MS/MS, 15 μl of the peptide solutions from the digestion supernatant was diluted with 30 μL in 5% formic acid, loaded onto the column, and washed with 30 μL of 5% formic acid. Peptides were eluted with 2.0 μL methanol/H_2O/formic acid (50/49/1, v/v/v) directly into a precoated borosilicate nanoelectrospray needles (EconoTip™, New Objective, USA). MS/MS of peptides generated by in-gel digestion was performed by nano-ESI on a Q-TOF2 mass spectrometer. The source temperature was 80 °C. A potential of 1 kV was applied to the precoated borosilicate nanoelectrospray needles in the ion source combined with a nitrogen back-pressure of 0–5 psi to produce a stable flow rate (10–30 nL/min). The mass spectrometer operated in an automatic data-dependent MS/MS to collect ion signals from the eluted peptides. In this mode, the most abundant peptide ion peak with doubly or triply charged ion in a full scan mass spectrum (m/z 400–1500) was selected as the precursor ion. Finally, an MS/MS spectrum was recorded to confirm the sequence of the precursor ion using collision-induced dissociation (CID) with a relative collision energy dependant on molecular weight. The cone voltage was 40 V. The quadrupole analyzer was used to select precursor ions for fragmentation in the hexapole collision cell. The collision gas was Ar at a pressure of $6–7\times10^{-5}$ mbar and the collision energy was 20–30 V. Product ions were analyzed using an orthogonal TOF analyzer, fitted with a reflector, a micro-channel plate detector and a time-to-digital converter. The data were processed using a Mass Lynx Windows NT PC system.

To identify the protein, peptide masses from MALDI-TOF MS were matched with the theoretical molecular weight of peptides for proteins in the NCBI database using MASCOT software. Also, all MS/MS spectra recorded on tryptic peptides derived from spot were searched against protein sequences from NCBInr and EST databases using the MASCOT search program (www.matrixscience.com).

Fluorescence imaging for CLIC1 localization

To determine the intracellular distribution of overexpressed CLIC1, the cells overexpressing GFP tagged CLIC1 on coverglass-bottom dish (SPL) were stained by 100 nM Mitotracker Red CMXRos and

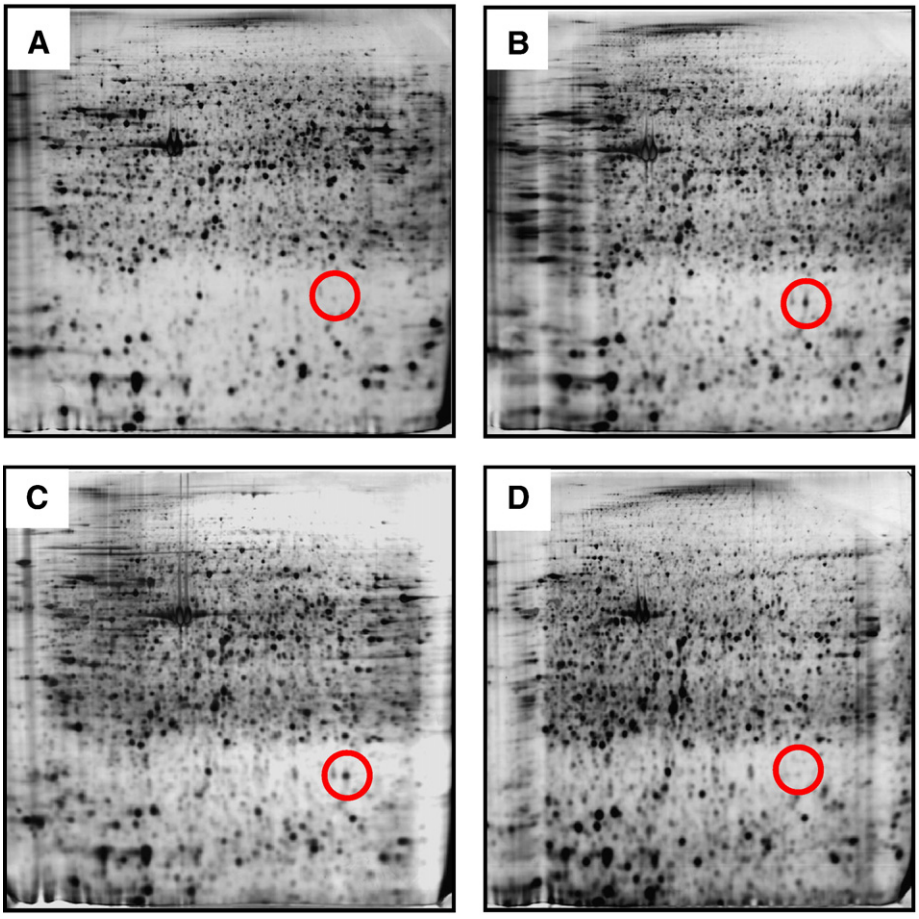

Fig. 1. Two-dimensional gel electrophoresis profiles of the proteins from C3H10T1/2 cells. C3H10T1/2 cells were transduced with control (A and D), Wnt-1a (B), or -10b (C) retrovirus and proteins were isolated as described in Materials and methods. Cells in (D) were treated with adipogenic medium containing insulin, dexamethasone, and IBMX. Red circle indicates protein whose expression was found to increase upon transduction with Wnt-1a and -10b retrovirus but to disappear after treatment with adipogenic medium. MALDI-TOF-MS analysis revealed that this spot corresponds to CLIC1.

visualized under a confocal scanning laser microscope (LSM-510 META, Carl Zeiss, Jena, Germany) with an 40× C-Apochromat objective water immersion using the 505–530 nm band-pass and 560–615 nm band-pass filter for colocalization of CLIC1 with mitochondria. For nuclear staining, the cells were stained with nuclear binding dye 4′,6-diamidino-2-phenylindole dihydrochloride (DAPI, Sigma-Aldrich, St. Louis, MO).

Measurement of mitochondrial membrane potential

Mitochondrial membrane potential was measured using the dye tetramethyl rhodamine ethyl ester (TMRE). The cells were loaded with 150 nM TMRE (Invitrogen) after 3 times washing with Normal-tyrode solution for 20–25 min at 37 °C. TMRE is rapidly taken up by live cells and preferentially distributes into negatively charged cellular compartments, because of its positive charge. The cells were excited by Argon and He/Ne laser sources in appropriate wavelength, and the images were acquired under a confocal scanning laser microscope (LSM-510 META) using 505–530 nm band-pass and >560 nm long-pass filter specifically for mitochondrial membrane potential measurement. The regions of interest were visualized every 17 s via time-series function using LSM-510 META software (Carl Zeiss). The fluorescence intensity was adjusted for stable state in 582 nm through FL-2 channel, and the effect of carboxyl cyanide p-trifluoromethoxy phenylhydrazone (FCCP) on the ratio of TMRE fluorescence in mitochondria relative to that surrounding cytosol was calculated and analyzed using Cell Quest Pro version 5.2.1 (Becton Dickinson) to quantify mitochondrial depolarization.

Measurement of plasma membrane Cl^- channel activities

Whole-cell recordings were performed on C3H10T1/2 cells transduced with pMSCV-CLIC1-IRES-GFP or MSCV-GFP retrovirus using protocols as described previously [8,18]. The pipette solution contained 140 mM KCl, 1.2 mM $MgCl_2$, 5 mM EGTA, 10 mM HEPES, and pH 7.2, with KOH. The bath solution contained 130 mM NaCl, 4.8 mM, KCl, 1.2 mM $MgCl_2$, 1.2 mM NaH_2PO_4, 10 mM HEPES, 12.5 mM glucose, 1 mM $CaCl_2$, bovine albumin (0.5 mg/ml, fraction V, Sigma), and pH 7.4, with NaOH. After establishing the whole-cell configuration, basal currents and volume activated Cl^- currents were measured. In order to identify the CLIC1-mediated currents, R(+)−[(6,7-Dichloro-2-cyclopentyl-2,3-dihydro-2-methyl-1-oxo-1H-inden-5-yl)-oxy]acetic acid (IAA-94), an inhibitor of CLIC1 Cl^- channel activity [8], was applied during basal current recording. To confirm the whole-cell configurations for Cl^- channel measurement, volume-activated Cl^- currents that are natively expressed C3H10T1/2 cells were activated by applying a hypotonic bath solution (260 mOsm). The hypotonic bath solution was made by reducing NaCl concentration. Currents were digitized and analyzed using an AxoScope 8.1 system and a Digidata 1322A AC/DC converter. Mean currents were normalized as current densities (pA/pF).

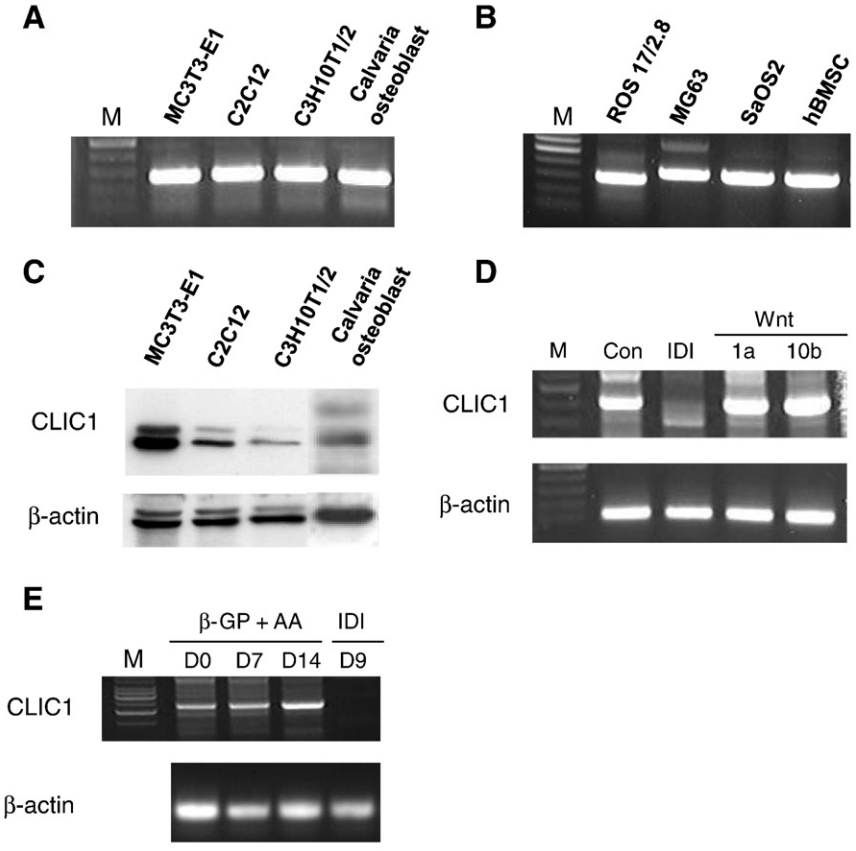

Fig. 2. Endogenous expression of CLIC1. (A) RT-PCR analysis of CLIC1 in mouse cells of mesenchymal origin. mRNA coding for mouse CLIC1 was detected by RT-PCR analysis from total RNA prepared from mouse osteoblastic MC3T3-E1, myoblastic C2C12, pluripotent mesenchymal C3H10T1/2 cells, and primary calvarial osteoblasts. (B) RT-PCR analysis of CLIC1 in different osteoblasts. CLIC1 mRNA was detected from total RNA prepared from rat osteoblastic ROS 17/2.8, human osteoblastic MG63 and SaOS2 cells, and primary human bone marrow stromal cells (hBMSC). (C) Western blot analysis of cellular expression of CLIC1. Cell lysates from confluent cultures of indicated cells were analyzed by SDS-polyacrylamide gel electrophoresis (SDS-PAGE) and Western blotting using anti-CLIC1 antibody. (D) RT-PCR analysis of CLIC1 from C3H10T1/2 cells with control virus at basal state (Con) and after treatment with adipogenic medium containing insulin, dexamethasone and IBMX for 14 days (IDI), and after transduction with either Wnt-1a or Wnt-10b retrovirus (D). (E) RT-PCR analysis of CLIC1 from MC3T3-E1 cells at basal (D0), on day 7 (D7) or day 14 (D14) after culture in osteogenic medium containing 50 μg/ml ascorbic acid and 10 mM of β-glycerophosphate (β-GP + AA) or after treatment with adipogenic medium (IDI) for 9 days (D9). M, 100 bp ladder.

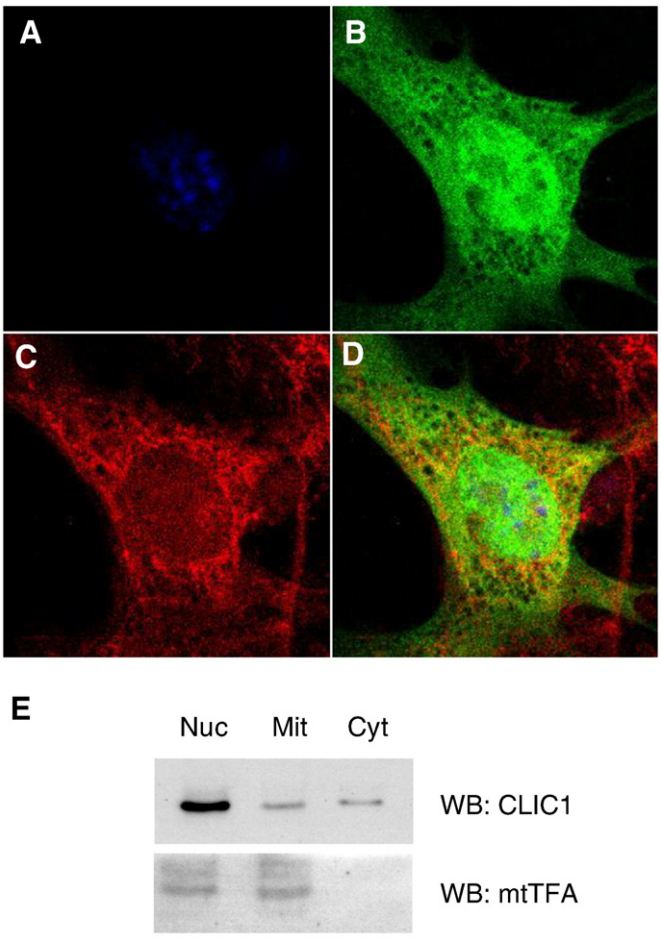

Fig. 3. Subcellular localization of CLIC1. C3H10T1/2 cells were transiently transfected with pCLIC1-EGFP and evaluated under the confocal microscope. (A) DAPI staining. (B) Localization of CLIC1 tagged with GFP. (C) Localization of mitochondria stained with MitoTracker Red. (D) Superimposed image shows partial colocalization of CLIC1 and mitochondria. (E) Western blots of subcellular fractions isolated from the cells. Indicated subcellular fractions were analyzed by SDS-polyacrylamide gel electrophoresis (SDS-PAGE) and Western blotting using anti-CLIC1 or anti-mtTFA (mitochondrial transcription factor A) antibody. Nuc, nuclear fraction; Mit, mitochondrial fraction; Cyt, cytosolic fraction.

Statistical analysis

All data are presented as mean ± SD. The data were analyzed by one-way ANOVA. When the ANOVA performed over all groups indicated a significant difference among the groups, statistical difference between two groups was subsequently evaluated by Student–Newman–Keuls multiple comparison test. A p value <0.05 was considered significant for all statistical analyses.

Results

Induction of CLIC1 after osteoblastogenic differentiation by canonical Wnt signaling

To identify candidate proteins that could play a pivotal role in the differentiation of mesenchymal cells, we attempted to identify spots in two-dimensional gel electrophoresis that are increased in osteoblastic differentiation but decreased during adipogenesis. We have transduced C3H10T1/2 cells with Wnt-1A or Wnt-10b retrovirus for osteoblastic differentiation and induced adipogenesis using adipogenic medium. Six spots were identified to fit these criteria and were further characterized by MALDI-TOF-MS and PDQuest software (Table 3). Fig. 1 shows an example of a silver stained two-dimensional gel electrophoresis images.

Among the 6 proteins we identified in Table 2, we decided to further characterize the role of CLIC1 in osteoblastogenesis because its expression was completely shut-down during adipogenesis, although either Wnt-1a or -10b increased the CLIC1 level less than 2-fold (inside circles in Fig. 1).

Expression of CLIC1 in osteoblasts

We first studied the expression of CLIC1 in various cell lines. Reverse transcription PCR analysis showed that expected cDNA fragments corresponding to mouse CLIC1 (275 bp) were clearly amplified from RNA isolated from mouse osteoblastic MC3T3-E1, myoblastic C2C12, embryonic mesenchymal C3H10T1/2, and primary mouse calvarial cells (Fig. 2A). In addition, we could also identify the mRNA expression of CLIC1 from rat osteoblastic ROS 17/2.8 cells (300 bp), human osteoblastic (MG63 and SaOS2) and primary bone marrow stromal cells (346 bp) (Fig. 2B).

Western blot analysis of protein extracts from these mesenchymal cell lines also revealed prominent signals of CLIC1 expression at 27 kDa (Fig. 2C). We were also able to identify the corresponding band from lysates of mouse primary calvarial cells (Fig. 2C).

To further confirm the results obtained from the 2-D gel analysis, we have transduced the C3H10T1/2 cells with retrovirus encoding Wnt-1a or 10b and examined the change in endogenous expression of CLIC1. As shown in Fig. 2D, the mRNA expression of CLIC1 was increased by overexpression of Wnt-1a or -10b, suggesting that these Wnt signaling enhances the expression of CLIC1 at the transcriptional level. In addition, when we examined the mRNA levels after treatment

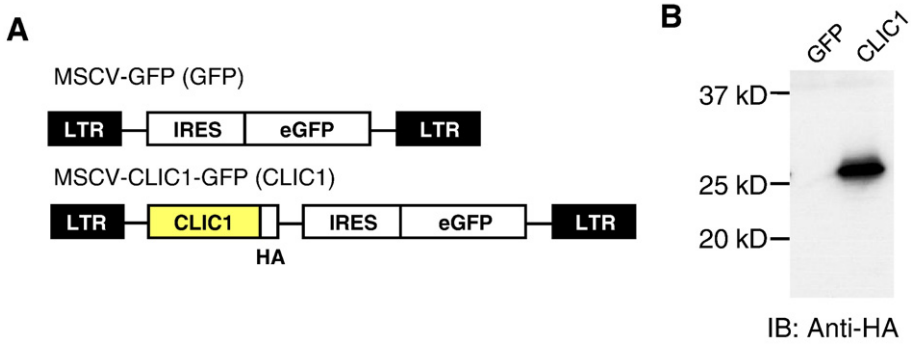

Fig. 4. Retroviral transduction of CLIC1 into C3H10T1/2 cells. (A) Schematic diagram of the retroviral construct used in this study. The solid rectangles represent Moloney murine leukemia virus long terminal repeats (LTR). HA, hemagglutinin epitope; IRES, internal ribosomal entry site of the encephalomyocarditis virus; GFP, green fluorescent protein gene. (B) Western blot analysis of total cell lysates from C3H10T1/2 cells. Cell lysates from confluent cultures were analyzed by SDS-PAGE and western blotting with anti-HA antibody. A band of ~27 kDa, corresponding to the CLIC1 was detected in cells carrying the CLIC1 but not in cells harboring GFP only (GFP).

with osteogenic or adipogenic medium, the expression level of CLIC1 is increased upon treatment of osteogenic medium, whereas it almost disappeared in adipogenic condition (Fig. 2E), confirming the initial proteomic data.

We next studied the localization of CLIC1 expression within the C3H10T1/2 cells. However, immunohistochemical analysis of C3H10T1/2 cells using commercial antibody against CLIC1 failed to detect the endogenous CLIC1 (data not shown). Therefore, we overexpressed CLIC1 by transient transfection of pCLIC1-EGFP, a fusion construct containing GFP at the C-terminal of CLIC1. As shown in Fig. 3B, the fluorescence was localized mainly in nucleus but substantial expression was also found in vesiculo-cytoplasmic area. When we stained the mitochondria with Mitotracker Red CMXRos (Fig. 3C), substantial overlap between CLIC1 and mitochondria was identified (Fig. 3D). Western blot analysis for the subfractions of the cell lysates also demonstrated predominant expression of CLIC1 in nucleus. Although we could detect modest mitochondrial contamination of nuclear fraction (mtTFA reactive band in nuclear fraction), it is clear that appreciable amount of CLIC1 is expressed in mitochondria as well as cytoplasmic area, consistent with the fluorescence study (Fig. 3E).

Overexpression of CLIC1 resulted in hyperpolarization of mitochondrial membrane potential

Next we studied the functional consequences of CLIC1 overexpression in mesenchymal C3H10T1/2 cells. Towards this end, the CLIC1 cDNA with a 3′ HA tag was introduced into the pMSCV-IRES-GFP retroviral vector under the transcriptional control of the **MSCV**-long terminal repeat and upstream of an IRES-GFP expression cassette, thereby allowing the co-expression of GFP with CLIC1 from a single bicistronic mRNA (Fig. 4A). Western blot analysis using an antibody that recognizes the HA tag (Fig. 4B) demonstrated a band of approximately 27 kDa, corresponding to mouse CLIC1 in cells carrying the retrovirus encoding CLIC1 but not in cells harboring GFP only. We then examined whether the retroviral overexpression of CLIC1 in C3H10T1/2 cells induces a Cl^- channel activity in the plasma membrane. Examples of whole-cell current tracings are presented Fig. 5A and B, and summarized results are shown in Fig. 5C. A clear volume activated Cl^- channel activity induced by hypotonic bath solution was observed in both mock-GFP and CLIC1-overexpressed cells. However, neither overexpression of CLIC1 nor treatment with the CLIC1 inhibitor IAA-94 evoked discernable changes in the whole-cell current measurements, suggesting that the overexpressed CLIC1 does not function as plasma membrane Cl^- channel at least in resting state. Given that the CLIC1 is distributed in cytoplasmic region but also partly overlapped with mitochondria in these cells, we next studied whether CLIC1 overexpression affects mitochondrial membrane potential. For this experiment, we loaded the cells with TMRE and analyzed the fluorescence using FACS (Fig. 6A). As shown in Fig. 6B, the percent change in the TMRE intensity after treatment with FCCP, a classical uncoupler of oxidative phosphorylation (Fig. 6A), was significantly increased by retroviral overexpression of CLIC1 in C3H10T1/2, suggesting that the mitochondrial membrane was significantly hyperpolarized by CLIC overexpression (Fig. 6B). We were also able to confirm the FACS results when we directly observe the TMRE intensity from the cells using confocal microscopy (Fig. 6C).

Effects of CLIC1 overexpression enhances osteoblastic differentiation in C3H10T1/2 cells

We next investigated whether CLIC1 plays a role in the differentiation of pluripotent mesenchymal cells. Culture of C3H10T1/2 cells in osteogenic medium for 21 days exhibited typical induction of ALP activity (Fig. 7A). Overexpression of CLIC1 by retrovirus transduction in this condition resulted in significant

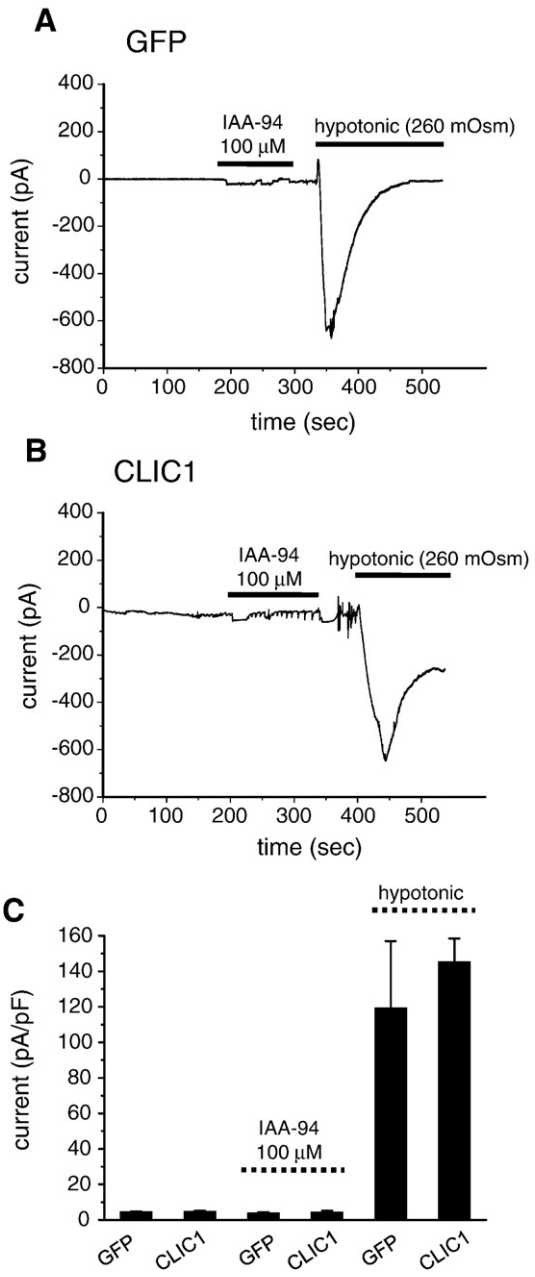

Fig. 5. Measurement of plasma membrane Cl^- channel activities. Whole-cell recordings were performed on C3H10T1/2 cells transduced with pMSCV-CLIC1-IRES-GFP (CLIC1) or MSCV-GFP (GFP) retrovirus as described in Materials and methods. Representative examples of whole-cell current tracings are presented in panels A and B, and summarized results of three experiments are shown in panel C. Neither overexpression of CLIC1 nor treatment with the CLIC1 inhibitor IAA-94 evoked discernable changes in the whole-cell current measurements. A volume activated Cl^- channel activity induced by hypotonic bath solution was measured at the end of each experiment to confirm the whole-cell configuration.

increase in ALP activity compared to the empty vector transduced cells (GFP). Consistent with the ALP activity result, increased mineralization was observed by the overexpression of CLIC1 (Fig. 7B). Moreover, CLIC1 overexpression increased mRNA level of osterix, ALP and osteocalcin (OC, Fig. 7C). Since osteocalcin is a downstream target of Runx2, the key transcription factor for osteoblast differentiation, we then studied whether CLIC1 overexpression enhances Runx2 transcriptional activity. 1.3 kb OG2 promoter harbors 3 Runx2 binding sites (OSE2 elements) allowing it to assess Runx2 promoter activity. However, as shown in Fig. 7D, the Runx2-induced reporter in C3H10T1/2 cells was not changed by the overexpression of CLIC1.

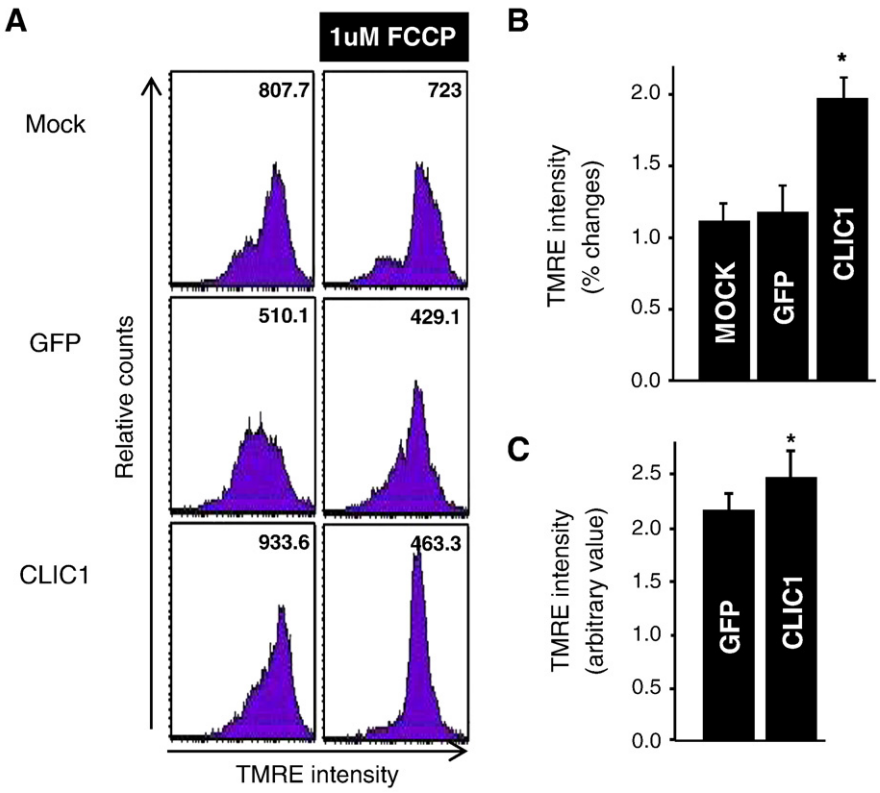

Fig. 6. Overexpression of CLIC1 induces hyperpolarization of mitochondrial membrane potential. (A) Representative histograms obtained from FACS analysis of C3H10T1/2 cells loaded with TMRE. C3H10T1/2 cells with mock treatment, transduced with empty retrovirus (GFP), or CLIC1 retrovirus were stained with fluorescent dye TMRE and analyzed by FACS before and after treatment with FCCP. Results are representative data from at least three independent experiments. (B) Quantitative results of FACS analysis. Percent change of TMRE intensity before and after treatment with FCCP is shown. *$p<0.05$ vs. Mock or GFP. (C) Quantitative results of TMRE intensity from C3H10T1/2 cells estimated using confocal microscope. Data are presented as mean ± SEM, *$p<0.05$ vs. GFP.

Collectively, these results suggest that CLIC1 expression enhances osteoblastic differentiation and mineralization of C3H10T1/2 cells, although the molecular mechanism is not clear.

Inhibition of ALP activity by siRNA of CLIC1

To further confirm the role of CLIC1 in osteoblastic differentiation of C3H10T1/2 cells, we established small interfering RNA duplexes (siRNA)-mediated knock-down of CLIC1 using a retrovirus-based system (pSIREN-RetroQ-CLIC1). We have generated 3 different plasmid vectors targeting different region of the mRNA. However, only pCLIC1-siRNA753 showed significant reduction in CLIC1 expression after stable transduction verified by Western blot analysis (Fig. 8A). The mitochondrial membrane potential as measured by FCCP-induced TMRE intensity changes showed corresponding reduction in cells transduced with pCLIC1-siRNA753 (Fig. 8B) although the difference was marginally significant ($p=0.05$). When the cells with siRNA were treated with β–glycerophosphate and ascorbic acid to induce osteoblastic differentiation, C3H10T1/2 cells stably transduced with pCLIC-siRNA753 exhibited significant reduction in both ALP staining (Fig. 8C) as well as ALP activities (Fig. 8D) whereas the cells with control retrovirus or other siRNA retrovirus did not. These results suggest the important role of CLIC1 in the osteoblastic differentiation of murine mesenchymal progenitors. *In vitro* knock-down of CLIC1 did not affect cell proliferation and cellular morphology (data not shown).

Discussion

In this study, we have shown that osteoblasts from various sources express CLIC1 and overexpression of CLIC1 leads to enhanced osteoblastic differentiation from mesenchymal progenitor cells. Moreover, *in vitro* knock-down of CLIC1 using siRNA resulted in attenuation of ALP activities.

CLIC1 belongs to a family of channel proteins and has been only recently characterized. Although its expression in wide variety of tissue has been reported, abundant expression in osteoblasts has never been documented. Another chloride channel, CLC-7, has been reported to be highly expressed in osteoclasts [19]. The expression level of CLIC1 increased after osteoblastogenic stimuli with Wnt signaling, including Wnt-1a or -10b, all canonical Wnt activators. Moreover, its expression is almost shut-down in adipogenic stimuli with adipogenic cocktail, which prompted us to further characterize the function of this molecule. We were also able to confirm the initial proteomic results with RT-PCR analysis. Given that osteoblastogenesis vs. adipogenesis is reciprocally regulated, the opposite direction of expression level by these two differentiation stimuli suggested its role in the lineage allocation or facilitation of differentiation to a certain direction.

We found that the CLIC1 primarily localized in nuclear membrane and cytoplasm including mitochondria. The functional role of nuclear CLIC1 has not been fully investigated. However, it could be expected that the chloride channel activity of nuclear CLIC1 could be associated with accumulation of Cl^-, which could modify the microenvironment of the nucleus with subsequent alteration of gene expression profile. In addition, it is possible that nuclear CLIC1 could physically interact with other nuclear proteins as was reported in the case of CLIC4 which binds with actin, tubulin, dynamin and AKAPs [20,21], thereby contributing to physiological functions. Although CLIC1 was originally identified as a nuclear channel protein (NCC27) in CHO cells, recent studies showed that its distribution is not exclusively in the nucleus [8] but substantial expression was also found in vesicular-cytoplasmic

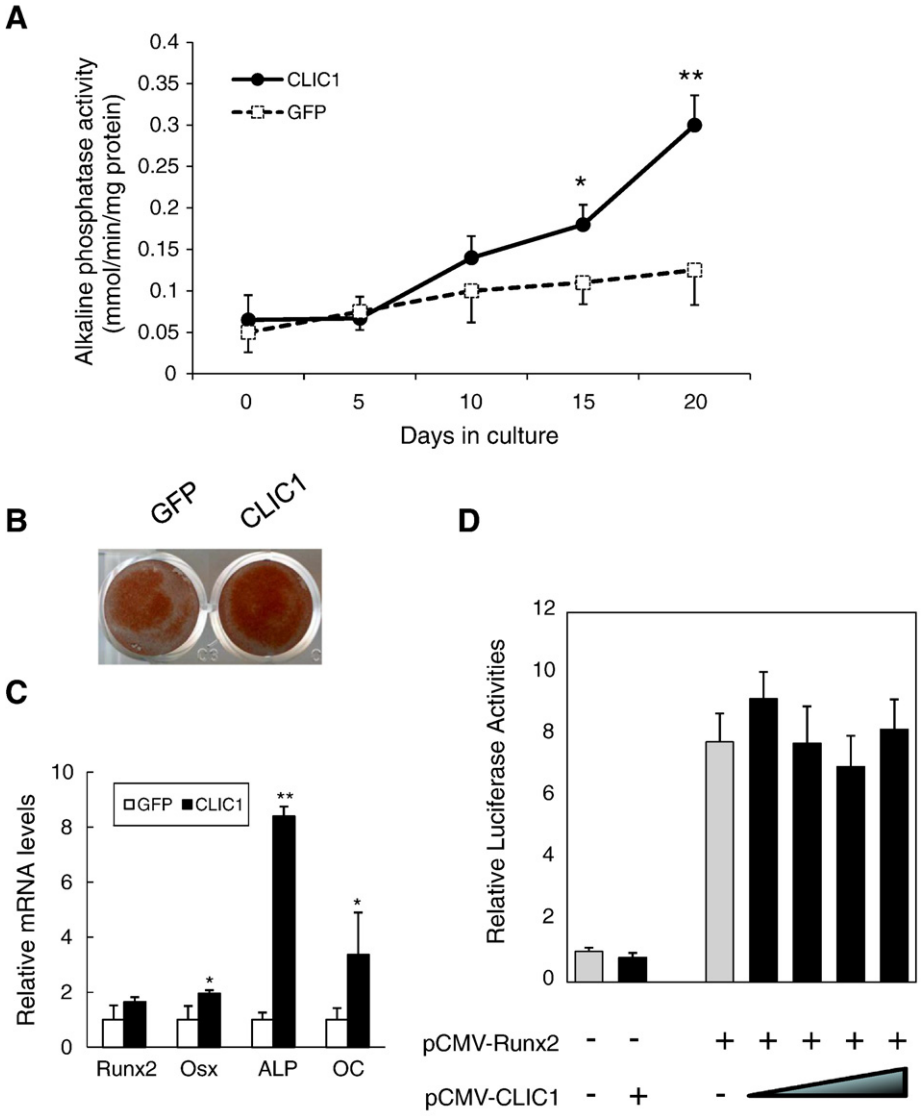

Fig. 7. Effect of CLIC1 overexpression on osteoblastic differentiation of C3H10T1/2 cells. C3H10T1/2 cells transduced with CLIC1 retrovirus or control virus (GFP) were seeded at 70–80% density in 24-well plate and grown for 21 days in DMEM/F12 containing 10% FBS, ascorbic acid (50 mg/ml), and β-glycerophosphate (10 mM) for 21 days. (A) Alkaline phosphatase activity was determined and normalized to protein content. The results are representative of three independent experiments performed in triplicate. Each bar represents means ± S.D. *$p<0.05$ **$p<0.01$ vs. vehicle. (B) Matrix mineralization was evaluated by Alizarin Red staining as described in Materials and methods. (C) Total RNA was extracted from C3H10T1/2 cells and quantitative real-time RT-PCR analysis for Runx2, osterix, ALP and osteocalcin was performed as described in Materials and methods. Values are presented as means ± S.E. *$p<0.05$, **$p<0.01$ vs. GFP. (D) C3H10T1/2 cells were cotransfected with mouse osteocalcin OG2 reporter plasmid (-1.3OG2-Luc) and expression vectors for Runx2 and/or CLIC1 as indicated. Luciferase activities were assayed as described in Materials and methods. Values are presented as means ± S.D., and results are representative of three experiments, each performed in triplicate.

area, consistent with our data [22,23]. Moreover, mtCLIC, a mouse homologue of CLIC4, which shares 67% of homology with CLIC1, is primarily expressed in mitochondria [24], suggesting that CLIC1 may have a biological function in the mitochondria as well as in the nuclear membrane. Indeed, we found that overexpression of CLIC1 has resulted in hyperpolarization of mitochondrial membrane potential, estimated using the fluorescent dye TMRE. CLIC1 overexpression-mediated hyperpolarization was also confirmed by direct observation of the dye using confocal microscope. However, in contrast to the significant changes in mitochondrial membrane potential, over-expression of CLIC1 in C3H10T1/2 cells did not result in change in whole-cell current. The reason for the lack of effect on the whole-cell current is not clear. However, our data are in line with the report of Fan et al.[23], who also showed that expression of CLIC1 alone did not increase whole-cell conductance either at rest or in response to increased intracellular cAMP in Xenopus oocytes [25]. Although CLIC1 has been largely regarded as channel protein, the structure and stoichiometry of the integral membrane form are still not clear [26], whereas clear channel activity was demonstrated when overexpressed in CHO cells [27]. Moreover, regarding the channel selectivity, Singh et al. [28] recently showed that CLIC5, a member of CLIC intracellular channel family, is equally permeable to Na^+, K^+, and Cl^- and raised questions on the function of CLIC as a true chloride channel. Thus, it seems that there are still many uncertainties in the role of CLIC1 in the context of cell physiology.

In this study, we have clearly demonstrated that overexpression of CLIC1 enhances osteoblastic differentiation, including ALP activities and osteoblastic gene expression. Moreover, using a siRNA knock-down strategy, we demonstrated that ALP activities were attenuated by the introduction of siCLIC1 retrovirus. However, the molecular mechanism by which overexpression of CLIC1 leads to osteoblastic differentiation is not clear. In this regards, it is interesting to note a recent study which demonstrated that intracellular concentration of Cl^- could affect the Runx2 activity because Runx transcription factor

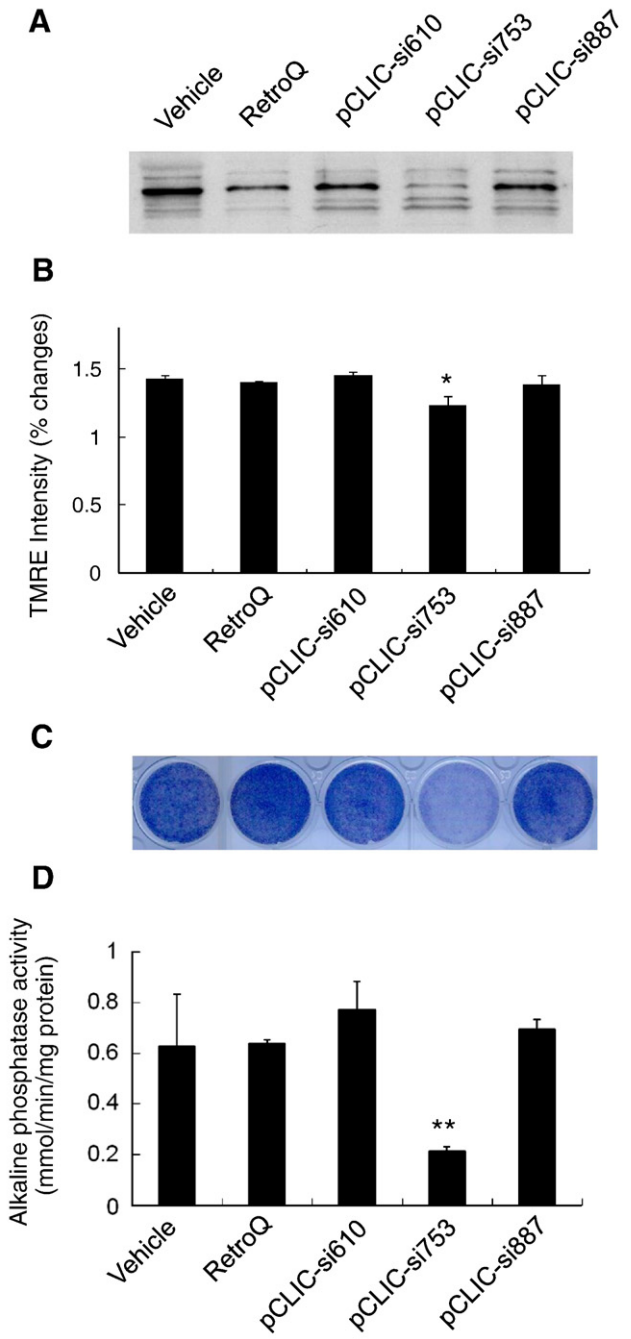

Fig. 8. Transduction of siRNA-CLIC1 inhibited osteoblastic differentiation of C3H10T1/2 cells. (A) Western blot analysis of cellular expression of CLIC1. Retrovirus expressing CLIC1 siRNA against CLIC1 mRNA (pCLIC-si610, -si753, or -si887) was prepared from pSIREN RetroQ vector and transduced to C3H10T1/2 cells. pCLIC1-siRNA753 showed significant reduction in CLIC1 expression after stable transduction. (B) Mitochondrial membrane potential measured by TMRE intensity changes. The cells were stained with fluorescent dye TMRE and analyzed by FACS before and after treatment with FCCP. Percent change of TMRE intensity is shown. (C and D) Alkaline phosphatase stain (C) and activities (D) of C3H10T1/2 cells with indicated retrovirus after culture in osteogenic medium containing ascorbic acid (50 mg/ml), and β-glycerophosphate (10 mM) for 21 days. $*p = 0.05$ $**p < 0.01$ vs. vehicle or RetroQ.

has been shown to be sensitive to Cl^- content in the nucleus [29]. Modulation of gene transcription by CLIC1 by way of alteration of chloride ion concentration has been also suggested previously [8]. However, in our hands, Runx2 transcriptional activity was not affected by the overexpression of CLIC1, suggesting that expression of CLIC1 in itself may not be sufficient to regulate Runx2-mediated transcription at the OSE2 element.

Given that the mitochondrial membrane is significantly hyperpolarized by CLIC1 overexpression, it may be plausible to expect that overexpressed CLIC1 could provide favorable condition for osteoblastic differentiation via adjusting ion current to support energy supplement during differentiation. In addition, it has been recently reported that sedlin, a cytoplasmic protein, is physically linked to CLIC1 thereby participating in the transportation of molecules across endoplasmic reticulum (ER)-to-Golgi intermediate compartment and regulates gene transcription [23]. In view of the fact that mutation of sedlin is reported in spondyloepiphyseal dysplasia tarda, an X-linked recessive skeletal disorder [30,31], it may be worth to pursue the role of physical interaction between CLIC1 and sedlin in the differentiation of osteoblasts.

In this study, we could identify the CLIC1 protein by proteomic screening of Wnt-responsive gene. However, we did not further pursue the regulation of CLIC1 by Wnt signaling. Nevertheless, we were able to identify the Tcf-responsive elements located in −6.9 kb and −1.0 kb of mouse and human CLIC1 promoter, respectively (data not shown), suggesting a possibility that CLIC1 may be a direct target of β-catenin/Tcf transcriptional control. Determining the molecular mechanisms by which the expression of CLIC1 is regulated will require further work.

In summary, we have identified CLIC1 through proteomic approach that responds to canonical Wnt signaling and enhances osteoblastic differentiation of mesenchymal progenitor cells. Further clarification of its physiologic role in osteoblasts as well as regulation mechanism may help to discover new targets for bone formation.

Acknowledgments

This work was supported by a grant from Seoul National University Hospital (grant # 03-2006-0100) and a grant from MarineBio Technology Project funded by Ministry of Land, Transport and Maritime Affairs of Korean government. MGL was supported by the grant R11-2007-040-01001-0 from the Korea Science and Engineering Foundation, Ministry of Education, Science and Technology, Korea.

References

[1] Cadigan KM, Nusse R. Wnt signaling: a common theme in animal development. Genes Dev 1997;11:3286–305.
[2] Gong Y, Slee RB, Fukai N, Rawadi G, Roman-Roman S, Reginato AM, et al. LDL receptor-related protein 5 (LRP5) affects bone accrual and eye development. Cell 2001;107:513–23.
[3] Little RD, Recker RR, Johnson ML. High bone density due to a mutation in LDL-receptor-related protein 5. N Engl J Med 2002;347:943–4 author reply 943-4.
[4] Bradbury JM, Niemeyer CC, Dale TC, Edwards PA. Alterations of the growth characteristics of the fibroblast cell line C3H 10T1/2 by members of the Wnt gene family. Oncogene 1994;9:2597–603.
[5] Rawadi G, Vayssiere B, Dunn F, Baron R, Roman-Roman S. BMP-2 controls alkaline phosphatase expression and osteoblast mineralization by a Wnt autocrine loop. J Bone Miner Res 2003;18:1842–53.
[6] Ross SE, Hemati N, Longo KA, Bennett CN, Lucas PC, Erickson RL, et al. Inhibition of adipogenesis by Wnt signaling. Science 2000;289:950–3.
[7] Longo KA, Wright WS, Kang S, Gerin I, Chiang SH, Lucas PC, et al. Wnt10b inhibits development of white and brown adipose tissues. J Biol Chem 2004;279:35503–9.
[8] Valenzuela SM, Martin DK, Por SB, Robbins JM, Warton K, Bootcov MR, et al. Molecular cloning and expression of a chloride ion channel of cell nuclei. J Biol Chem 1997;272:12575–82.
[9] Ashley RH. Challenging accepted ion channel biology: p64 and the CLIC family of putative intracellular anion channel proteins (Review). Mol Membr Biol 2003;20:1–11.
[10] Tonini R, Ferroni A, Valenzuela SM, Warton K, Campbell TJ, Breit SN, et al. Functional characterization of the NCC27 nuclear protein in stable transfected CHO-K1 cells. FASEB J 2000;14:1171–8.
[11] Furlan F, Lecanda F, Screen J, Civitelli R. Proliferation, differentiation and apoptosis in connexin43-null osteoblasts. Cell Commun Adhes 2001;8:367–71.
[12] Yoo JJ, Song WS, Koo KH, Yoon KS, Kim HJ. Osteogenic abilities of bone marrow stromal cells are not defective in patients with osteonecrosis. Int Orthop 2008.
[13] Pittenger MF, Mackay AM, Beck SC, Jaiswal RK, Douglas R, Mosca JD, et al. Multilineage potential of adult human mesenchymal stem cells. Science 1999;284:143–7.
[14] Zhang R, Ducy P, Karsenty G. 1,25-dihydroxyvitamin D3 inhibits Osteocalcin expression in mouse through an indirect mechanism. J Biol Chem 1997;272:110–6.

[15] Li X, Liu P, Liu W, Maye P, Zhang J, Zhang Y, et al. Dkk2 has a role in terminal osteoblast differentiation and mineralized matrix formation. Nat Genet 2005;37:945–52.
[16] Kim SK, Yoo JI, Cho BK, Hong SJ, Kim YK, Moon JA, et al. Elevation of CRABP-I in the cerebrospinal fluid of patients with Moyamoya disease. Stroke 2003;34:2835–41.
[17] Jensen ON, Mortensen P, Vorm O, Mann M. Automation of matrix-assisted laser desorption/ionization mass spectrometry using fuzzy logic feedback control. Anal Chem 1997;69:1706–14.
[18] Lee JH, Richter W, Namkung W, Kim KH, Kim E, Conti M, et al. Dynamic regulation of cystic fibrosis transmembrane conductance regulator by competitive interactions of molecular adaptors. J Biol Chem 2007;282:10414–22.
[19] Schaller S, Henriksen K, Sveigaard C, Heegaard AM, Helix N, Stahlhut M, et al. The chloride channel inhibitor NS3736 [corrected] prevents bone resorption in ovariectomized rats without changing bone formation. J Bone Miner Res 2004;19:1144–53.
[20] Suginta W, Karoulias N, Aitken A, Ashley RH. Chloride intracellular channel protein CLIC4 (p64H1) binds directly to brain dynamin I in a complex containing actin, tubulin and 14-3-3 isoforms. Biochem J 2001;359:55–64.
[21] Berryman MA, Goldenring JR. CLIC4 is enriched at cell–cell junctions and colocalizes with AKAP350 at the centrosome and midbody of cultured mammalian cells. Cell Motil Cytoskeleton 2003;56:159–72.
[22] Tulk BM, Edwards JC. NCC27, a homolog of intracellular Cl- channel p64, is expressed in brush border of renal proximal tubule. Am J Physiol 1998;274:F1140–9.
[23] Fan L, Yu W, Zhu X. Interaction of Sedlin with chloride intracellular channel proteins. FEBS Lett 2003;540:77–80.
[24] Fernandez-Salas E, Sagar M, Cheng C, Yuspa SH, Weinberg WC. p53 and tumor necrosis factor alpha regulate the expression of a mitochondrial chloride channel protein. J Biol Chem 1999;274:36488–97.
[25] Edwards JC. The CLIC1 chloride channel is regulated by the cystic fibrosis transmembrane conductance regulator when expressed in Xenopus oocytes. J Membr Biol 2006;213:39–46.
[26] Littler DR, Harrop SJ, Fairlie WD, Brown LJ, Pankhurst GJ, Pankhurst S, et al. The intracellular chloride ion channel protein CLIC1 undergoes a redox-controlled structural transition. J Biol Chem 2004;279:9298–305.
[27] Warton K, Tonini R, Fairlie WD, Matthews JM, Valenzuela SM, Qiu MR, et al. Recombinant CLIC1 (NCC27) assembles in lipid bilayers via a pH-dependent two-state process to form chloride ion channels with identical characteristics to those observed in Chinese hamster ovary cells expressing CLIC1. J Biol Chem 2002;277:26003–11.
[28] Singh H, Cousin MA, Ashley RH. Functional reconstitution of mammalian "chloride intracellular channels" CLIC1, CLIC4 and CLIC5 reveals differential regulation by cytoskeletal actin. FEBS J 2007;274:6306–16.
[29] Backstrom S, Wolf-Watz M, Grundstrom C, Hard T, Grundstrom T, Sauer UH. The RUNX1 Runt domain at 1.25A resolution: a structural switch and specifically bound chloride ions modulate DNA binding. J Mol Biol 2002;322:259–72.
[30] Gedeon AK, Colley A, Jamieson R, Thompson EM, Rogers J, Sillence D, et al. Identification of the gene (SEDL) causing X-linked spondyloepiphyseal dysplasia tarda. Nat Genet 1999;22:400–4.
[31] Gedeon AK, Tiller GE, Le Merrer M, Heuertz S, Tranebjaerg L, Chitayat D, et al. The molecular basis of X-linked spondyloepiphyseal dysplasia tarda. Am J Hum Genet 2001;68:1386–97.